

Slow passage through a transcritical bifurcation in piecewise linear differential systems: canard explosion and enhanced delay

A. Pérez-Cervera*

A. E. Teruel†

September 20, 2023

Abstract

In this paper we analyse the phenomenon of the slow passage through a transcritical bifurcation with special emphasis in the maximal delay $z_d(\lambda, \varepsilon)$ as a function of the bifurcation parameter λ and the singular parameter ε . We quantify the maximal delay by constructing a piecewise linear (PWL) transcritical normal form and studying the dynamics near the slow-manifolds. Our findings encompass all potential maximum delay behaviours within the range of parameters, allowing us to identify: i) the trivial scenario where the maximal delay tends to zero with the singular parameter; ii) the singular scenario where $z_d(\lambda, \varepsilon)$ is not bounded, and also iii) the transitional scenario where the maximal delay tends to a positive finite value as the singular parameter goes to zero. Moreover, building upon the concepts by A. Vidal and J.P. Françoise (Int. J. Bifurc. Chaos Appl. 2012), we construct a PWL system combining symmetrically two transcritical normal forms in such a way it shows periodic behaviour. As the parameter λ changes, the system presents a non-bounded canard explosion leading to an enhanced delay phenomenon at the critical value. Our understanding of the maximal delay $z_d(\lambda, \varepsilon)$ of a single normal form, allows us to determine both, the amplitude of the canard cycles and, in the enhanced delay case, the increasing of the amplitude for each passage.

1 Introduction

Slow passage or delayed bifurcations are dynamical phenomena that typically occur in ordinary differential equations with slow drifting parameters. In particular, consider a one parametric family of differential equations $\dot{\mathbf{x}} = \mathbf{f}(\mathbf{x}, y)$ and assume slowly dynamics for the parameter y , that is $y = y_0 + \varepsilon t$ with $0 < \varepsilon \ll 1$, what can also be expressed as the differential equation

$$\begin{aligned}\dot{\mathbf{x}} &= \mathbf{f}(\mathbf{x}, y), \\ \dot{y} &= \varepsilon.\end{aligned}\tag{1}$$

Due to the time-scale separation, differential system (1) is commonly referred to as a slow-fast system, whereby \mathbf{x} represents the fast variable and y represents the slow variable. For such slow-fast systems, one aims to describe the flow of the full system (1) for $\varepsilon > 0$ starting from the flow of the fast subsystem, that is, system (1) with $\varepsilon = 0$.

Following Fenichel's results [12, 20], compact normally hyperbolic invariant manifolds of the fast subsystem persist as slow manifolds for $\varepsilon > 0$, and they are located at a $O(\varepsilon)$ Hausdorff distance of the original manifold. Fenichel's theory also describes the behaviour of the flow along the slow manifold and surrounding it.

In particular, equilibrium points of the differential equation $\dot{\mathbf{x}} = \mathbf{f}(\mathbf{x}, y)$ give rise to a manifold of equilibria of the fast subsystem (1) called the critical manifold, $\mathcal{S}_0 = \{(\mathbf{x}, y) : \mathbf{f}(\mathbf{x}, y) = 0\}$. While the equilibrium point of the equation is hyperbolic, the critical manifold is normally hyperbolic and persists as a slow manifold \mathcal{S}_ε for $\varepsilon > 0$. Therefore, the behaviour of the flow of full system (1), on and around the slow manifold \mathcal{S}_ε , is described by the Fenichel's results. However, when the equilibrium point loses its hyperbolicity at a bifurcation by changing stability, branches of the slow manifold with different stability properties usually appear. In this scenario, the evolution of

Keywords: Piecewise linear systems, dynamic bifurcations, slow passage, transcritical bifurcation, enhanced delay.

*Departament de Matemàtiques. Universitat Politècnica de Catalunya, Barcelona, Spain

†Departament de Matemàtiques i Informàtica & IAC3, Universitat de les Illes Balears, Palma de Mallorca, Spain

the slow manifolds and of the flow around them is not predicted by Fenichel's theory and depends on the interplay between the slow manifolds. Under suitable conditions, there exist trajectories that evolve close to the repelling slow manifold for a time after the bifurcation, which is regarded as a delay in the loss of stability. Therefore, canard trajectories [2, 6] appear as a transitional dynamical objects in the loss of stability phenomenon.

The delay in the loss of stability has been analyzed through different bifurcations including the Hopf bifurcation [26, 27, 1, 11, 19], and as of particular interest for this paper, the transcritical bifurcation [22, 18, 10, 21, 23, 24, 17, 9]. Transcritical singularities, have been studied by means of different methods including the blow up technique [22], the discretization of the flow [10] and more recently by local linearization along the critical manifold [21].

In this paper, we approach the slow passage through a transcritical bifurcation by constructing a piecewise linear (PWL) canonical system. PWL systems have been widely used to reproduce non linear behaviour and to provide complementary understanding about some bifurcations [25, 4, 30]. In addition, the PWL approach has recently been used to study slow-fast dynamics. Indeed, approaching slow-fast systems by PWL systems has a significant advantage: it straightforwardly provides canonical slow manifolds, which indeed, are locally affin subspaces. Since the slow manifold is an essential part of the skeleton of slow-fast dynamics, the PWL approach allows for a treatable but still meaningful problem as it does not miss the salient features of their smooth counterpart (see for example [13, 8, 7, 5, 3]). Indeed, the PWL approach has been used recently to study delayed bifurcations, as for example the Hopf and the Homoclinic bifurcations [28, 29].

When studying the delay of the loss of stability, an important function quantifying such delay is the so-called way-in/way-out function. Consider a tubular δ -neighbourhood N_δ around the slow manifold. Given an orbit, the way-in/way-out function relates the distance between the bifurcation point and the inner point of the orbit through N_δ , with the distance between the bifurcation point and the outer point of the orbit through N_δ . Roughly speaking, the way-in/way-out function relates the ratio of repulsion and attraction of the branches of the slow manifold. The asymptotic value of the way-in/way-out function is known as the maximal delay.

By analysing the slow passage through a transcritical bifurcation through the PWL framework, we achieve a full control on the way-in/way-out function and on the maximal delay. By means of this understanding we describe well-known situations as, for example, how the maximal delay goes to zero as the singular parameter goes to zero. However, we also tackle non trivial behaviours as for instance the degenerate situation in which the maximal delay is unbounded. Moreover, our results also cover the transitional regime from the trivial to the degenerate case. In this intermediate regime the maximal delay is finite when the singular parameter tends to zero.

As we discussed before, this transitional regime is related with canard trajectories. In [15] slow-fast systems with two (or more) transcritical bifurcations are constructed in such a way one can have canard cycles allowing to study canard regimes and enhanced delay. Following the ideas introduced in [15], we combine two of our PWL units exhibiting slow passage through a transcritical bifurcation. As a result, the orbits leaving from the repelling slow manifold of one unit connect with the stable slow manifold of the other one. In this way, we generate oscillatory behaviour by alternating the passage through one PWL unit to the other. In this scenario we show the existence of a one parameter family of limit cycles undergoing a canard explosion up to a critical value in which the amplitude of the canard cycles tends to infinity. When the parameter takes such a critical value, we also show the occurrence of the enhanced delay phenomenon in which each passage through each unit increases the delay of the next passage.

Our paper is organised as follows: in Section 2, we present our PWL normal form for the transcritical bifurcation and provide expressions for the canonical slow manifolds. In Section 3, we state the main results of the manuscript. In Section 4 we build a PWL system exhibiting two transcritical bifurcations and apply our previous results to analyse the canard explosions and the enhanced delay occurring at this system. Finally in Section 5 we provide the proof of the main results. The paper ends with one appendix A where we provide the local expressions for the flows of our PWL normal form.

2 A PWL normal form for a transcritical bifurcation

Let us consider the continuous piecewise linear differential system

$$\begin{aligned} x' &= |x| - |y| + \lambda\varepsilon, \\ y' &= \varepsilon, \end{aligned} \tag{2}$$

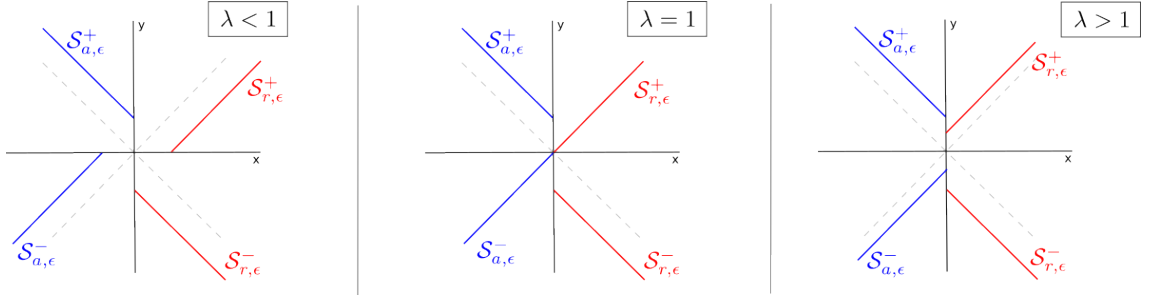


Figure 1: **Configuration of the slow manifolds.** Representation of the attracting slow manifold $\mathcal{S}_{a,\epsilon}^\pm$ (blue lines) and the repelling slow manifold $\mathcal{S}_{r,\epsilon}^\pm$ (red lines) of system (2) depending on the values of λ , see expressions (5)-(6).

with parameters $0 \leq \varepsilon \ll 1$ and $\lambda > 0$. The Lipschitz character of the vector field ensures the uniqueness of the solutions of the initial condition problem. Hence, let $\varphi(t; (x_0, y_0), \lambda, \varepsilon)$ denote the solution of (2) with initial condition (x_0, y_0) . Even if the system (2) is globally non-linear, when restricted to any of the four quadrants, Q_k with $k \in \{1, 2, 3, 4\}$, it becomes linear. Therefore, local expressions for the flow can be easily obtained, see Eq. (17)-(18).

For $\varepsilon = 0$ the equilibrium points of system (2) define the critical manifold

$$\mathcal{S}_0 = \{(x, y) : |x| = |y|\}. \quad (3)$$

All the equilibrium points in \mathcal{S}_0 , except the origin, are normally hyperbolic. Indeed, its respective Jacobian matrix has an eigenvalue with real part equal to zero and another eigenvalue equal to ± 1 . Hence, the critical manifold \mathcal{S}_0 , is the union of: (i) four normally hyperbolic branches, two attracting $\mathcal{S}_{a,0}^\pm$ and two repelling $\mathcal{S}_{r,0}^\pm$

$$\mathcal{S}_{a,0}^\pm = \{(x, y) : y = \mp x, x < 0\}, \quad \mathcal{S}_{r,0}^\pm = \{(x, y) : y = \mp x, x > 0\}; \quad (4)$$

and (ii) the point $(0, 0)$ which is not normally hyperbolic. We note that the subscript a, r in the slow manifold indicates attracting or repelling and the superscript \pm corresponds to the sign of the y variable.

Let us now study the perturbed system ($\varepsilon > 0$). In this case, Fenichel's theory [12, 20] implies that outside of a small neighbourhood of $(0, 0)$, the different branches of the critical manifold persist as slow manifolds. By computing the eigenspace associated with the slow eigenvalue of system (2), we can obtain analytical expressions for canonical slow manifolds [31]. In that way we obtain the following expressions for the two canonical stable slow manifolds

$$\begin{aligned} \mathcal{S}_{a,\varepsilon}^- &= \{(x, y) : y = x + \varepsilon(1 - \lambda), \quad x < \min\{0, \varepsilon(\lambda - 1)\}\}, \\ \mathcal{S}_{a,\varepsilon}^+ &= \{(x, y) : y = -x + \varepsilon(1 + \lambda), \quad x < 0\}. \end{aligned} \quad (5)$$

and for the two canonical unstable slow manifolds

$$\begin{aligned} \mathcal{S}_{r,\varepsilon}^- &= \{(x, y) : y = -x - \varepsilon(1 + \lambda), \quad x < 0\}, \\ \mathcal{S}_{r,\varepsilon}^+ &= \{(x, y) : y = x - \varepsilon(1 - \lambda), \quad x > \max\{0, \varepsilon(1 - \lambda)\}\}, \end{aligned} \quad (6)$$

each of them perturbing from its respective branch of the critical manifold given in (4) (see Fig. 1).

3 Statement of the main results

In this section, for system (2) and $\varepsilon > 0$, we characterise how the trajectories in a small neighbourhood of the attracting slow manifold $\mathcal{S}_{a,\varepsilon}^-$ continue beyond the transcritical bifurcation at the origin. To this aim, we consider a tubular neighbourhood $N(\delta)$ of radius δ , with $\delta > 2\varepsilon$, around both the attracting $\mathcal{S}_{a,\varepsilon}^-$ and the repelling $\mathcal{S}_{r,\varepsilon}^+$ slow manifolds. By considering this tube, one can study the relationship between the point $\mathbf{p}_i = (x_i, y_i)^T$ in which an orbit γ enters $N(\delta)$ and the point $\mathbf{p}_o = (x_o, y_o)^T$ at which this orbit leaves $N(\delta)$. Indeed, the relationship between y_o and $|y_i|$ defines a function, usually denoted as the way-in/way-out function. Typically, the graph of the way-in/way-out function approaches asymptotically a value corresponding with the ordinate of the

exit point of the attracting slow manifold $\mathcal{S}_{a,\varepsilon}^-$. This asymptotic value, which is a function of the parameters λ, ε , is denoted as the *maximal delay* $z_d(\lambda, \varepsilon)$. We quantify thorough the paper the delay in the loss of stability in terms of this maximal delay.

Our results cover the cases $0 < \lambda < 1$, $\lambda = 1$ and $\lambda > 1$. First, in Theorem 3.1, we offer a PWL perspective of the classical results by Krupa and Szmolyan in [22] for fixed $\lambda \neq 1$. Additionally, in Theorem 3.3 we interpret their results in terms of the maximal delay $z_d(\lambda, \varepsilon)$ and show that in these cases $\lim_{\varepsilon \searrow 0} z_d(\lambda, \varepsilon) = 0$. Moreover, in Theorem 3.6, we also study the degenerate case $\lambda = 1$ proving that for this value the maximal delay is unbounded.

In order to bring together these two regimes we explore solutions where, instead of λ being a fixed parameter, we consider $\lambda(\varepsilon) = 1 \pm e^{-c/\varepsilon}$ with $c \in \mathbb{R}^+$. For such a value of λ , in Theorem 3.8, we prove that the system: (i) exhibits trajectories with canard segments; and (ii) its maximal delay satisfies $\lim_{\varepsilon \searrow 0} z_d(\lambda, \varepsilon) = c$ (see Fig. 2 and Remark 3.9).

3.1 Slow passage for fixed λ

Similarly as in [22], we define the crossing sections

$$\begin{aligned}\Delta^{\text{in}} &= \{(-\rho, -\rho + \varepsilon(1 - \lambda) + r) : |r| < \delta\}, \\ \Delta_a^{\text{out}} &= \{(-\rho, \rho + \varepsilon(1 + \lambda) + r) : |r| < \delta\}, \\ \Delta_e^{\text{out}} &= \{(\rho, r) : |r| < \delta\},\end{aligned}$$

where $\rho > 0$ and $|\delta| \ll 1$ and the transition maps

$$\Pi_e : \Delta^{\text{in}} \rightarrow \Delta_e^{\text{out}}, \quad \Pi_a : \Delta^{\text{in}} \rightarrow \Delta_a^{\text{out}},$$

from Δ^{in} to Δ_e^{out} and Δ_a^{out} , respectively. Moreover, we define as \mathbf{p}_a^- the point in the boundary of $\mathcal{S}_{a,\varepsilon}^-$ given by

$$\mathbf{p}_a^- = (x, x + \varepsilon(1 - \lambda)), \quad \text{with } x = \min\{0, \varepsilon(\lambda - 1)\}, \quad (7)$$

and $\gamma_{\mathbf{p}_a^-}$ as the orbit through \mathbf{p}_a^- . Therefore our PWL view of the results in [22] are as follows:

Theorem 3.1 *Fixed $\lambda > 0$, there exists $\varepsilon_0 > 0$ such that the following statements hold for $\varepsilon \in (0, \varepsilon_0]$.*

- a) *If $\lambda > 1$ then the orbit $\gamma_{\mathbf{p}_a^-}$ passes through Δ_e^{out} at a point $(\rho, h(\varepsilon))$ where $h(\varepsilon) = O(\varepsilon \ln(\varepsilon))$. The section Δ^{in} is mapped by Π_a to an interval containing $\gamma_{\mathbf{p}_a^-} \cap \Delta_e^{\text{out}}$ of size $O(e^{-c/\varepsilon})$ where c is a positive constant.*
- b) *If $\lambda < 1$ then, Δ^{in} is mapped by Π_e to an interval containing $\mathcal{S}_{a,\varepsilon}^+ \cap \Delta_a^{\text{out}}$ of size $O(e^{-c/\varepsilon})$ where c is a positive constant.*

Remark 3.2 *The dynamical behaviour described in Theorem 3.1 is completely comparable to that for the transcritical bifurcation in the smooth context appearing in Theorem 2.1 in [22]. Nevertheless, for $\lambda > 1$, there is a quantitative difference in the size of the ordinate $h(\varepsilon)$, while in [22] it is order $O(\sqrt{\varepsilon})$, here it is order $O(\varepsilon |\ln(\varepsilon)|)$. We note that in both cases $h(\varepsilon)$ tends to zero with ε .*

Theorem 3.1 describes the evolution of the slow manifold $\mathcal{S}_{a,\varepsilon}^-$, and of the orbits surrounding it, beyond a neighbourhood of the origin. It is also interesting to describe this evolution in terms of the delay in the loss of stability, or more concretely in terms of the maximal delay $z_d(\lambda, \varepsilon)$. In the next result we board this question by revisiting Theorem 3.1 in terms of the maximal delay.

Theorem 3.3 *Fixed $\lambda > \ln(2)$, there exists $\varepsilon_0 > 0$ such that the following statements hold for $\varepsilon \in (0, \varepsilon_0]$.*

- a) *If $\lambda > 1$, the maximal delay satisfies that $z_d(\lambda, \varepsilon) \leq O(\varepsilon \ln(|\varepsilon|))$.*
- b) *If $\lambda < 1$, there exists a differentiable function $C(\lambda)$ such that the maximal delay satisfies that $z_d(\lambda, \varepsilon) \leq \varepsilon(\lambda + C(\lambda))$.*

Remark 3.4 *From Theorem 3.3, it follows that fixed $\lambda \neq 1$, $\lim_{\varepsilon \searrow 0} z_d(\lambda, \varepsilon) = 0$ (see Fig. 2).*

Remark 3.5 The value of ε_0 appearing in Theorem 3.1 and in Theorem 3.3 is a function of λ . As we show in next Section 5 (see Equations (12) and (14)), we obtain the following explicit expression for $\varepsilon_0(\lambda)$

$$\varepsilon_0(\lambda) = \begin{cases} \frac{e^{1-C(\lambda)}}{C(\lambda)-1} & \lambda < 1, \\ \min \left\{ \left(\frac{2(e^{\lambda-1}-1)}{\rho+\lambda-1} \right)^{\frac{1}{2}}, \frac{\rho}{2e^{\lambda-1}-(\lambda+1)} \right\} & \lambda > 1, \end{cases}$$

where $\rho \in \mathbb{R}$ and $C(\lambda)$ is a differentiable function. From this expression and since $\lim_{\lambda \searrow 1} C(\lambda) = +\infty$ (see Lemma 5.3) it follows that $\varepsilon_0(\lambda)$ shrinks to 0 as λ tends to 1. Therefore, $\lambda = 1$ corresponds with a degenerate case.

In the next result, we describe the behaviour of the flow surrounding $\mathcal{S}_{a,\varepsilon}^-$ and $\mathcal{S}_{r,\varepsilon}^+$ in the degenerate case $\lambda = 1$.

Theorem 3.6 For $\lambda = 1$ and $\varepsilon > 0$, the attracting branch $\mathcal{S}_{a,\varepsilon}^-$ and the repelling branch $\mathcal{S}_{r,\varepsilon}^+$ of the slow manifold connect at the origin. Therefore, the maximal delay is unbounded. Moreover, let $N(\delta)$ be a tubular neighbourhood of the slow manifold $\mathcal{S}_{a,\varepsilon}^- \cup \mathcal{S}_{r,\varepsilon}^+$ of radius δ , then the graph of the way-in/way-out function is located between the lines $y = x + \delta$ and $y = x - \delta$. Consequently, the way-in/way-out function tends asymptotically to infinity and therefore, is not bounded.

Remark 3.7 In the Remark 2.2 in [22], the authors assure the existence of a function $\lambda_c(\sqrt{\varepsilon})$ with $\lambda_c(0) = 1$ and such that, for $\lambda = \lambda_c(\sqrt{\varepsilon})$, the slow manifold $\mathcal{S}_{a,\varepsilon}^-$ extends to $\mathcal{S}_{r,\varepsilon}^+$ for ε sufficiently small. From our Theorem 3.6, it follows that in the PWL setup, the function $\lambda_c(\sqrt{\varepsilon})$ is identically 1. Moreover, the authors in [22] claim that “for values of λ exponentially close to $\lambda_c(\sqrt{\varepsilon})$ the slow manifold $\mathcal{S}_{a,\varepsilon}^-$ can follow $\mathcal{S}_{r,\varepsilon}^+$ over an $O(1)$ -distance before being repelled”. This last statement motivates the next section.

3.2 Slow passage for $\lambda(\varepsilon)$

In this Section we study how the maximal delay $z_d(\lambda, \varepsilon)$ behaves for values of λ exponentially close to the degenerate value $\lambda = 1$. In particular we explore $\lambda(\varepsilon) = 1 \pm e^{-c/\varepsilon}$.

Theorem 3.8 Let c and ε be positive constants and ε small enough.

- a) If $\lambda = 1 - e^{-\frac{c}{\varepsilon}}$, then for $\tau = \tau_1 + \tau_2$ where $\tau_1 = e^{-\frac{c}{\varepsilon}} + O\left(e^{-\frac{2c}{\varepsilon}}\right)$ and $\tau_2 = \frac{c}{\varepsilon} + \ln\left(\frac{c}{2\varepsilon}\right)$, it follows that $\varphi(\tau; \mathbf{p}_a^-) = (0 + X(\varepsilon), c + Y(\varepsilon))^T$ where $X(\varepsilon) = \varepsilon \ln\left(\frac{c}{2\varepsilon}\right) + O(\varepsilon e^{-\frac{c}{\varepsilon}})$ and $Y(\varepsilon) = \varepsilon \ln\left(\frac{c}{2\varepsilon}\right) + O\left(e^{-\frac{c}{\varepsilon}}\right)$.
- b) If $\lambda = 1 + e^{-\frac{c}{\varepsilon}}$, then for $\tau = \tau_1 + \tau_2$ where $\tau_1 = e^{-\frac{c}{\varepsilon}}$ and $\tau_2 = \frac{c}{\varepsilon} + \ln\left(\frac{c}{2\varepsilon}\right)$, it follows that $\varphi(\tau; \mathbf{p}_a^-) = (2c + X(\varepsilon), c + Y(\varepsilon))^T$ where $X(\varepsilon) = \varepsilon \ln\left(\frac{c}{2\varepsilon}\right) + O(\varepsilon e^{-\frac{c}{\varepsilon}})$ and $Y(\varepsilon) = \varepsilon \ln\left(\frac{c}{2\varepsilon}\right)$.

Remark 3.9 As a consequence of Theorem 3.8, when λ is $O(e^{-\frac{c}{\varepsilon}})$ close to 1, the maximal delay satisfies $z_d(\lambda, \varepsilon) = c + h(\varepsilon)$ and $\lim_{\varepsilon \searrow 0} z_d(\lambda(\varepsilon), \varepsilon) = c$ (see Fig. 2).

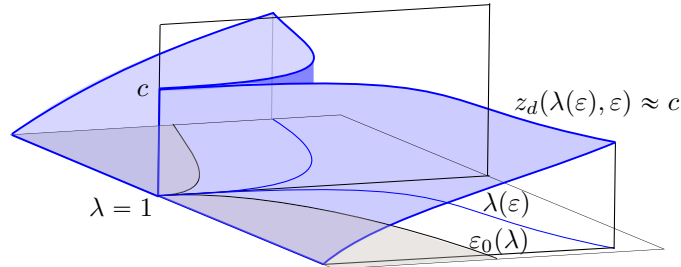


Figure 2: **Sketch of the maximal delay function z_d over the (λ, ε) -plane.** The shadowed region corresponds with $\varepsilon < \varepsilon_0(\lambda)$ in Remark 3.5 and shows that for fixed $\lambda \neq 1$, $\lim_{\varepsilon \searrow 0} z_d(\lambda, \varepsilon) = 0$. The blue curve on the domain corresponds with the parameter curve $\lambda(\varepsilon) = 1 \pm e^{-\frac{c}{\varepsilon}}$ showing that $\lim_{\varepsilon \searrow 0} z_d(\lambda(\varepsilon), \varepsilon) = c$.

4 Canard explosion and enhanced delay

In this Section we study an application of the slow passage through a transcritical bifurcation inspired by the model analyzed in [15, 32]. To that aim, we consider the two parameter (λ, ε) PWL system given by

$$\begin{cases} \begin{cases} \dot{x} = |x + 1/2| - |y - 1/2| + \lambda\varepsilon, \\ \dot{y} = \varepsilon(y - x), \end{cases} & y - x \geq 0, \\ \begin{cases} \dot{x} = -|x - 1/2| + |y + 1/2| - \lambda\varepsilon, \\ \dot{y} = \varepsilon(y - x), \end{cases} & y - x \leq 0. \end{cases} \quad (8)$$

As one can see, system (8) consists in two different passages through transcritical bifurcations which are locally identical to the one we have previously analyzed in Section 3. Indeed, the two transcritical bifurcations are located at $\mathbf{p}_- = (-1/2, 1/2)$ and $\mathbf{p}_+ = (1/2, -1/2)$ which are on the straight lines $y - x = 1$ and $y - x = -1$, respectively. Therefore, as long as the trajectories remain close to these lines, the system (8) locally shows comparable dynamics as the one generated by the system (2). Consequently, we consider each passage separately and then we use the local dynamics to describe the global flow.

The system (8) is formed by two copies of the system (2) studied previously, with a common boundary at the line $y - x = 0$. Even if for $\varepsilon = 0$ the vector field of system (8) is continuous, that is nevermore the case when $\varepsilon > 0$ because of the constant terms $\pm\lambda\varepsilon$ appearing in both subsystems. Because of this discontinuity, we follow Filippov's convention [14, 16] to define the vector field over the line $y = x$ and hence, for $\varepsilon > 0$ there exists a sliding segment S_l along the switching line $y = x$. This sliding segment is limited by the end points $\mathbf{e}_- = (-\frac{\lambda\varepsilon}{2}, -\frac{\lambda\varepsilon}{2})$ and $\mathbf{e}_+ = (\frac{\lambda\varepsilon}{2}, \frac{\lambda\varepsilon}{2})$, corresponding with boundary equilibrium points of system (8) in $y - x \geq 0$ and $y - x \leq 0$, respectively. Therefore, for every point of the phase plane but the sliding segment, there exists a unique orbit passing through it [16]. We also note that as the system is invariant under the change of variables $(x, y) \rightarrow (-x, -y)$, the orbits are symmetric with respect to the origin.

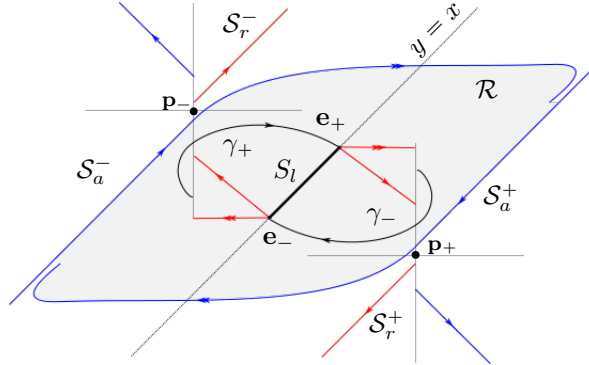


Figure 3: **Phase plane of system (8)** containing the following elements: (i) the attracting slow manifolds \mathcal{S}_a^\pm and the repelling slow manifolds \mathcal{S}_r^\pm associated to the transcritical bifurcation at points $\mathbf{p}_- = (-\frac{1}{2}, \frac{1}{2})$ and $\mathbf{p}_+ = (\frac{1}{2}, -\frac{1}{2})$; (ii) the positive invariant region \mathcal{R} (dashed area) which is limited by the attracting slow manifolds and contains the sliding segment S_l ; (iii) The boundary equilibrium points \mathbf{e}_+ and \mathbf{e}_- which are of node type, together with the fast eigenspace and the slow eigenspace (indicated with two and one arrows, respectively).

The local analysis around the transcritical bifurcation (see Theorem 3.3(a)), ensures that when $\lambda > 1$ the attracting slow manifold \mathcal{S}_a^- of the subsystem located in $y - x > 0$, leaves the neighbourhood of the repelling branch \mathcal{S}_r^- at a distance $O(\varepsilon|\ln(\varepsilon)|)$ above of the bifurcation point \mathbf{p}_- . Then, because of the symmetry, the orbit gets a neighbourhood of the attracting branch \mathcal{S}_a^+ of the subsystem in $y - x < 0$, passes through the bifurcation point \mathbf{p}_+ , follows the repelling branch \mathcal{S}_r^+ , and leaves it at a distance $O(\varepsilon|\ln(\varepsilon)|)$ below the point \mathbf{p}_+ . This behaviour gives rise to a positive invariant region \mathcal{R} containing the sliding segment S_l , see Figure 3.

Let γ_- be the orbit locally contained in $y - x < 0$ with \mathbf{e}_- as ω -limit set (resp. γ_+ the orbit locally contained in $y - x > 0$ with \mathbf{e}_+ as ω -limit set). We now discuss the behaviour of the orbits inside \mathcal{R} depending on the parameters λ, ε . For λ, ε values such that \mathbf{e}_+ is contained in the

α -limit set of γ_- , then by the symmetry of the flow it follows that $\mathbf{e}_- \in \alpha(\gamma_+)$. In consequence, there is a heteroclinic connection $\Gamma_h = \gamma_- \cup \gamma_+$ inside \mathcal{R} and containing the sliding segment S_l . Otherwise, the sliding segment S_l is a global attractor for the flow in \mathcal{R} , see Figure 3.

Let us now discuss about the stability of the heteroclinic connection Γ_h . First, we note that \mathbf{e}_- and \mathbf{e}_+ are locally repeller equilibrium points of node type, both having one fast eigenspace and one slow eigenspace, see Figure 3. For the critical values of the parameters λ, ε for which γ_+ contains the fast eigenspace of \mathbf{e}_- the heteroclinic cycle Γ_h appears and it is outside stable and inside unstable. Conversely, when γ_- does not contain the fast eigenspace of \mathbf{e}_+ then Γ_h is unstable both inside and outside. Specifically, the α -limit set of every orbit in a neighborhood of Γ_h is $\{\mathbf{e}_+, \mathbf{e}_-\}$. Therefore, since \mathcal{R} is a positive invariant region and $\{\mathbf{e}_+, \mathbf{e}_-\}$ are the α -limit set of any orbit in a neighborhood containing Γ_h , from the Poincaré-Bendixon Theorem we conclude that a stable limit cycle Γ surrounding Γ_h appears in region \mathcal{R} .

The limit cycle Γ borns with an amplitude A equal to the amplitude of Γ_h , that is, $A = O(\|\mathbf{e}_+ - \mathbf{e}_-\|) = O(\varepsilon\lambda)$. Furthermore, as ε decreases to zero, the limit cycle approaches the attracting slow manifold S_a^- and hence Γ tends to the boundary of region \mathcal{R} . Therefore, when λ is fixed and greater than 1, the attracting branch of the slow manifold S_a^- in $x - y < 0$, leaves the neighbourhood of the repelling branch S_r^- at a distance $z_d(\lambda, \varepsilon) = \varepsilon|\ln(\varepsilon)|$ from the bifurcation point \mathbf{p}_- . Therefore, the amplitude of Γ is $A = 1 + O(\varepsilon|\ln(\varepsilon)|)$. Furthermore, if we take $\lambda = 1 + e^{-\frac{\varepsilon}{2}}$ the attracting branch S_a^- follows for a time the repelling branch S_r^- , giving rise to a canard segment. Then S_a^- leaves the neighbourhood of S_r^- at a distance $z_d(\lambda, \varepsilon) = c + \varepsilon h(\varepsilon)$ from the bifurcation point, where $\varepsilon h(\varepsilon)$ tends to zero as $\varepsilon \rightarrow 0$ (see Theorem 3.8(b)). Consequently, Γ is a (headless) canard cycle with amplitude

$$A = 1 + 2c + 2\varepsilon h(\varepsilon), \quad (9)$$

where $c = -\varepsilon \ln(\lambda - 1)$. In Figure 4 we draw for the canard explosion taking place at $\lambda = 1$ for $\varepsilon = 0.02$ and $\varepsilon = 0.05$.

Expression (9) provides an explicit relation between the amplitude A of the canard cycle and the value of the parameter λ at which that canard cycle exists; that is $\lambda(A) = 1 + e^{-\frac{A-1}{2\varepsilon}}$. In this scenario we can measure the range of variation of the amplitude with respect to the parameter as

$$\frac{dA}{d\lambda} = -2\varepsilon e^{\frac{A-1}{2\varepsilon}}$$

which is exponentially big.

Remark 4.1 We conclude that system (8) presents a two parameter family of stable limit cycles $\Gamma_{\varepsilon, \lambda}$ for $\varepsilon > 0$ and $\lambda > 1$. Let $A(\varepsilon, \lambda)$ denote the amplitude of $\Gamma_{\varepsilon, \lambda}$.

Fixed ε_0 positive and small enough, the family of limit cycles appears for $\lambda_b = O(\varepsilon_0^{-1})$ at a bifurcation at which the sliding segment S_l changes its stability. The amplitude at the bifurcation is $A(\varepsilon_0, \lambda_b) = O(1)$. As λ decreases to 1 the amplitude of the limit cycles increases and the family overcomes a canard explosion, see Figure 4. At the canard explosion, from (9), the amplitude of

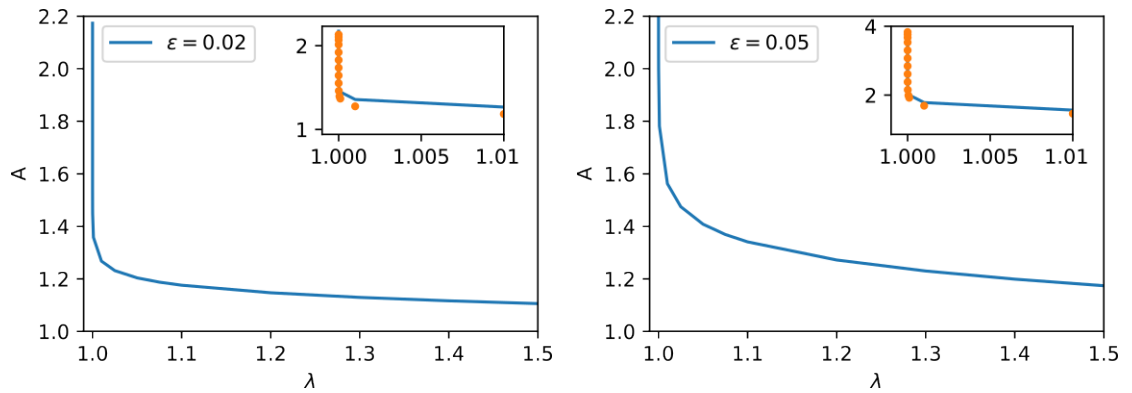


Figure 4: **Canard explosion occurring in system (8).** In the Figure we represent the amplitude of the canard cycle versus the parameter λ for $\varepsilon = 0.02$ (left) and $\varepsilon = 0.05$ (right). In both panels we draw an inset Figure showing the computed amplitude A of the canard explosion (blue line) and the theoretical prediction, see equation (9) (orange dots).

the canard cycles can be accurately approximated by $A(\varepsilon_0, \lambda) = 1 - 2\varepsilon_0 \ln(\lambda - 1)$ (see the orange points in the inset panels of Figure 4). From the previous expression of the amplitude we obtain the partial derivative $\frac{\partial A}{\partial \lambda}(\varepsilon_0, \lambda) = -\frac{2\varepsilon_0}{\lambda - 1}$. Hence, for λ exponentially close to 1, that is $\lambda = 1 + e^{-\frac{\varepsilon}{\varepsilon_0}}$, it follows that the amplitude of the canard cycle remains constant $A(\varepsilon_0, \lambda) = 1 + 2c$. Finally, its derivative $\frac{\partial A}{\partial \lambda}(\varepsilon_0, \lambda) = -2\varepsilon e^{\frac{\varepsilon}{\varepsilon_0}}$ is exponentially big.

On the other side, fixed $\lambda_0 > 1$, as ε decreases to zero, the amplitude of the limit cycles satisfies $A(\varepsilon, \lambda_0) = 1 + O(\varepsilon \ln(\varepsilon))$ where no dependence on λ_0 appears. The accuracy of this approximation is represented in Figure 5.

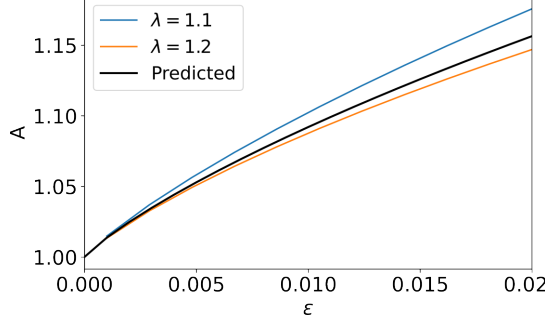


Figure 5: **Amplitude of the cycles for fixed λ .** In this Figure we show the validity of the theoretical approximation for the amplitude given by $A = 1 + 2\varepsilon |\ln(\varepsilon)|$ for two fixed values of λ .

When $\lambda = 1$, as a consequence of Theorem 3.6, it follows that the attracting slow manifold \mathcal{S}_a^- (resp. \mathcal{S}_a^+) connects with the repelling slow manifold \mathcal{S}_r^- (resp. \mathcal{S}_r^+) at the transcritical bifurcation point located at $\mathbf{p}_- = (-\frac{1}{2}, \frac{1}{2})$ (resp. $\mathbf{p}_+ = (\frac{1}{2}, -\frac{1}{2})$). Therefore, the previous mentioned invariant region \mathcal{R} becomes an unbounded invariant strip in the phase plane given by $-1 \leq y - x \leq 1$, that is, the region laterally limited by the union of the slow manifolds $\mathcal{S}_a^+ \cup \mathcal{S}_r^+$ (and also $\mathcal{S}_a^- \cup \mathcal{S}_r^-$). Moreover, since the amplitude of canard cycles tends to infinity as λ tends to 1^+ , we conclude that the canard explosion ends at a heteroclinic loop with the equilibrium points at infinity and with heteroclinic orbits given by $\mathcal{S}_a^+ \cup \mathbf{p}_+ \cup \mathcal{S}_r^+$ and $\mathcal{S}_a^- \cup \mathbf{p}_- \cup \mathcal{S}_r^-$.

As we now discuss, our understanding of the system allows us to provide theoretical predictions for the increase in each passage of the amplitude of the oscillatory behaviour existing in the invariant strip \mathcal{R} . Consider small amplitude tubular neighbourhoods along these four invariant manifolds and let us describe the dynamical behaviour of the orbits with respect to these tubular neighbourhoods. Consider an orbit which enters the tubular neighbourhood around \mathcal{S}_a^- at a point with ordinate $y_0 < \frac{1}{2}$. Then, Theorem 3.6 ensures that the orbit suffers a delay of magnitude $\frac{1}{2} - y_0$ after passing the transcritical bifurcation point, and leaves the neighbourhood of the repelling slow manifold \mathcal{S}_r^- at a point with ordinate $1 - y_0$. In a similar way, when an orbit gets inside the tubular neighbourhood around \mathcal{S}_a^+ with ordinate y_0 , it suffers a delay $\frac{1}{2} + y_0$ and leaves the neighbourhood of \mathcal{S}_r^+ with ordinate $-1 - y_0$. In particular, for ε small enough, if an orbit approaches \mathcal{S}_a^- with ordinate y_0 , then it suffers a first delay and leaves \mathcal{S}_r^- at $y_1 = 1 - y_0$, then approaching \mathcal{S}_a^+ with the same ordinate and, after a second delay, leaving \mathcal{S}_r^+ with ordinate $y_2 = -1 - y_1$, and then approaching again \mathcal{S}_a^- but now with ordinate $y_2 = -2 + y_0$. In this case, the orbit suffers a delay which is 2 units greater than the first delay. This phenomenon is called enhanced delay [15]. Finally, the orbit leaves the unstable slow manifold \mathcal{S}_r^- with ordinate $y_3 = 1 - y_2 = 3 - y_0$, and so on.

Remark 4.2 We conclude that, for sufficiently small ε , when an orbit approaches the attracting manifold with ordinate y_0 , at each passage through one transcritical bifurcation it undergoes an enhanced delay of magnitude equal 2 units, given rise to an oscillatory dynamical behaviour of increasing amplitude (see Fig. 6 left panel), and whose peaks and valleys follow the sequences $\{2k - 1 - y_0\}_{k=1}^\infty$, $\{-2k + y_0\}_{k=1}^\infty$, respectively (Fig. 6 right panel).

5 Proof of main results

In this Section, we provide the proof of the main results of our study. In these proofs, the local expression of the solution $\varphi(t; (x_0, y_0), \lambda, \varepsilon)$ of system (2) given in (17)-(18) plays a central role.

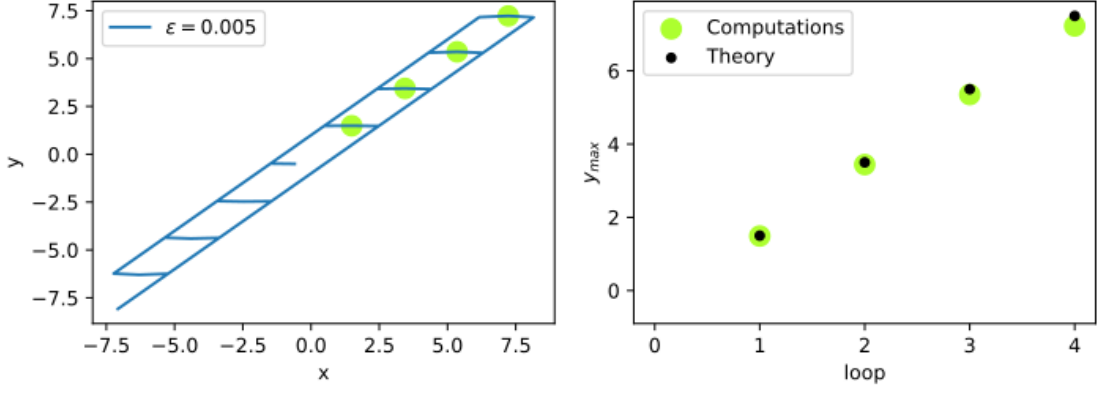


Figure 6: **Enhanced delay.** In this Figure we illustrate the phenomenon of enhanced delay for the system (8). In the left panel, we start a trajectory at $(x_0, y_0) = (-0.6, -0.5)$ and integrate numerically the system (8) for a time $t \approx 14001.12$ (in which it completes 4 complete loops). We observe how the maximum value for the y component (green dots) increases every loop thus showing the validity of the theoretical predictions in Remark 4.2. Indeed we computed $y_{\max} = \{1.49, 3.44, 5.35, 7.23\}$ (to be compared with $\{1.5, 3.5, 5.5, 7.5\}$). The accuracy of the theoretical prediction will increase as $\varepsilon \rightarrow 0$, however the numerical accuracy required checking this scenario is beyond our software.

However, throughout this Section, we omit the dependence of φ in λ, ε to maintain notation as simpler as possible.

5.1 Proof of Theorem 3.1

In the next Lemma we describe the evolution of the orbit passing through the point

$$\mathbf{p}_t = (0, \varepsilon\lambda), \quad (10)$$

where the flow of system (2) is tangent to the line $\{x = 0\}$. Hence, as we geometrically show in fig. 7(a) and next prove, this orbit delimits the set of orbits that intersect the quadrant Q_1 from that which do not.

Lemma 5.1 *Let $\varphi(t; \mathbf{p}_t)$ be the solution of system (2) with initial condition \mathbf{p}_t .*

- a) *For $t \geq -\lambda$, the solution $\varphi(t; \mathbf{p}_t)$ is contained in Q_4 , and $\varphi(-\lambda; \mathbf{p}_t) = (\varepsilon(\lambda-1) - \varepsilon(e^\lambda - 2), 0)^T$.*
- b) *For $\tau_t = \frac{\rho}{\varepsilon} + 1$ then, $d(\varphi(\tau_t; \mathbf{p}_t), \mathcal{S}_{a,\varepsilon}^+ \cap \Delta_a^{\text{out}}) = O(e^{-\frac{\rho}{\varepsilon}})$.*

Proof: The solution $\varphi(t; \mathbf{p}_t)$ is tangent to $\{x = 0\}$ at \mathbf{p}_t . In fact,

$$\varphi(t; \mathbf{p}_t) = \mathbf{p}_t + \begin{pmatrix} 0 \\ \varepsilon \end{pmatrix} t + \begin{pmatrix} -\varepsilon \\ 0 \end{pmatrix} \frac{t^2}{2} + O(t^3).$$

Therefore, $\varphi(t; \mathbf{p}_t)$ is locally contained in Q_4 . The time derivative of the first coordinate is negative for $t > 0$, since the second coordinate is always increasing, we conclude that the solution is contained in Q_4 for $t \geq 0$. Similarly, for $t < 0$ the first and the second coordinates of the solution decreases. As long as $t > -\lambda$, the second coordinate still positive, and hence it will be contained in Q_4 . To finish the proof of the statement (a) we compute $\varphi(-\lambda; \mathbf{p}_t)$ straightforwardly from the expression of the flow in Q_4 given in (17)-(18). The proof of the statement (b) in the Lemma follows directly from evaluating the flow in Q_4 at the corresponding times. \square

5.1.1 Case $\lambda < 1$

First, we enunciate the following Lemmas that will help us to determine, for a given $\lambda < 1$ value, the possible paths of the orbit starting at the point $\mathbf{p}_a^- = (\varepsilon(\lambda - 1), 0)^T$ given in (7). This orbit corresponds with the evolution of the attracting slow manifold $\mathcal{S}_{a,\varepsilon}^-$.

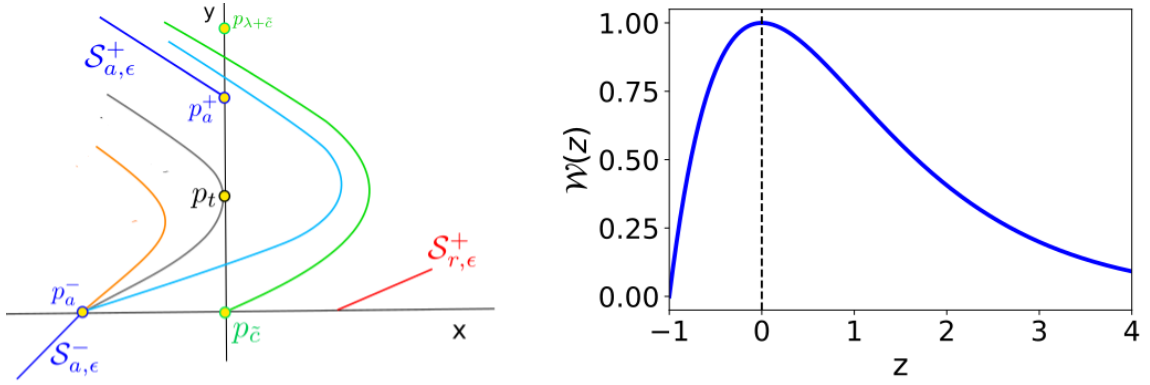


Figure 7: **Sketch of the possible behaviours of the flow through \mathbf{p}_a^- for $0 < \lambda < 1$.** (Left) The orbit through \mathbf{p}_t (grey curve for $\lambda = \ln(2)$) separates the orbits which are fully contained in Q_4 (orange curve for $\lambda \leq \ln(2)$) and the ones that also visit Q_1 (cyan curve for $\ln(2) < \lambda < 1$). The trajectories through the origin (green curve), also determine the maximal height at which it is possible to cross the y -axis. (Right) Graph of the map $\mathcal{W}(z)$ on the domain $[-1, \infty)$.

Lemma 5.2 *Let $\varphi(t; \mathbf{p}_a^-)$ be the solution of system (2) with initial condition at \mathbf{p}_a^- and assume $\lambda \in (0, \ln(2)]$.*

- a) *For $t \geq 0$, the solution $\varphi(t; \mathbf{p}_a^-)$ is contained in the quadrant Q_4 .*
- b) *For $\tau_a = \frac{\rho}{\epsilon} + 1 + \lambda$, then $d(\varphi(\tau_a, \mathbf{p}_a^-), \mathcal{S}_{a,\epsilon}^+ \cap \Delta_a^{out}) = O(e^{-\frac{\rho}{\epsilon}})$.*

Proof: When $\lambda \in (0, \ln(2)]$ the first coordinate of \mathbf{p}_a^- is less than the first coordinate of $\varphi(-\lambda; \mathbf{p}_t)$ see Lemma 5.1(a). Hence, the statement (a) follows as $\varphi(t; \mathbf{p}_t)$ is contained in Q_4 . The statement (b) follows straightforwardly from evaluating the flow in Q_4 at $t = \tau_a$. \square

In Lemma 5.2 we have shown that for $0 < \lambda \leq \ln(2)$, the solutions through \mathbf{p}_a^- is contained in Q_4 . Otherwise, for $\ln(2) < \lambda < 1$ the solution leaves Q_4 , and evolves through Q_1 before entering again Q_4 by crossing the y -axis, see Lemma 5.5. In the next Lemma, we provide an upper bound for the ordinate of such crossing. To that aim, we first define the functions $\mathcal{W}(z)$ and $C(\lambda)$ given by

$$\mathcal{W}(z) := (1+z)e^{-z} \quad \text{and} \quad \mathcal{W}(C(\lambda)) = \mathcal{W}(-\lambda), \quad (11)$$

where the graph of \mathcal{W} on the domain $[-1, +\infty)$ is depicted in fig. 7(b), and $C(\lambda)$ is implicitly well-defined and analytical in the domain $(0, 1)$. We straightforwardly conclude that $C'(\lambda) > 0$, $C(\lambda) > 1$ if $\lambda \geq \ln(2)$, $\lim_{\lambda \rightarrow 1} C(\lambda) = +\infty$, and $\lim_{\lambda \rightarrow 1} C'(\lambda) = +\infty$.

Lemma 5.3 *Consider $\lambda \in (0, 1)$ and let $C(\lambda)$ be the function implicitly defined in (11). The solution of system (2) with initial condition at the origin, $\varphi(t; \mathbf{0})$, is locally contained in Q_1 for $t \in (0, \lambda + C(\lambda))$ and $\varphi(\lambda + C(\lambda); \mathbf{0}) = (0, \epsilon(\lambda + C(\lambda)))^\top$.*

Proof: The vector field at the origin is given by $\epsilon(\lambda, 1)$, so that the solution with initial condition at the origin is contained in Q_1 for a sufficiently small time interval. From the local expression of the solution $\varphi(t; \mathbf{0})$ while in Q_1 , see (17), we obtain that $\varphi(t; \mathbf{0}) = ((\lambda - 1)\epsilon e^t + \epsilon t - (\lambda - 1)\epsilon, \epsilon t)$. Therefore, $\varphi(t, \mathbf{0})$ leaves Q_1 if there exists a positive value of t for which the first coordinate is 0. Equivalently, the solution leaves Q_1 if there exists $c > 0$ such that $(1 - \lambda)e^\lambda = (1 + c)e^{-c}$, where the time to escape is given by $t = \lambda + c$. From (11) it follows that $c = C(\lambda)$ which ends the proof. \square

In Lemma 5.3 we have obtained the point $\mathbf{p}_c = (0, \epsilon(\lambda + C(\lambda)))^\top$ whose y -coordinate gives an upper bound for the crossing of the y -axis. We note that since $C(\lambda)$ tends to ∞ as $\lambda \rightarrow 1$ and the second coordinate of the vector field is positive, reaching the attracting manifold $\mathcal{S}_{a,\epsilon}^+$ at an ordinate ρ introduces naturally a maximal value for ϵ as a function of λ . Consider the function $\epsilon_0 : (0, 1) \rightarrow \mathbb{R}^+$ given by

$$\epsilon_0(\lambda) = \frac{e^{1-C(\lambda)}}{C(\lambda) - 1}, \quad (12)$$

where $C(\lambda)$ is the analytical function implicitly given in (11). Straightforward computations show that

$$\lim_{\lambda \rightarrow 1} \varepsilon_0(\lambda) = 0, \quad \lim_{\lambda \rightarrow 1} \varepsilon'_0(\lambda) = -\infty.$$

In the next Lemma we study the evolution of the solution through \mathbf{p}_c after entering quadrant Q_4 .

Lemma 5.4 *Fix $\lambda \in (\ln(2), 1)$ and let $\varphi(t; \mathbf{p}_c)$ be the solution with initial condition at $\mathbf{p}_c = (0, \varepsilon(\lambda + C(\lambda)))^\top$.*

a) *For $t \geq 0$, the solution $\varphi(t; \mathbf{p}_c)$ is contained in the quadrant Q_4 .*

b) *Consider $0 < \varepsilon \leq \varepsilon_0(\lambda)$, for $\tau_c = \frac{\rho}{\varepsilon} + (C(\lambda) - 1)(e^{-\frac{\rho}{\varepsilon}} - 1)$, then $d(\varphi(\tau_c, \mathbf{p}_c), \mathcal{S}_{a,\varepsilon}^+ \cap \Delta_a^{\text{out}}) = O(e^{-\frac{\rho}{\varepsilon}})$.*

Proof: The solution with initial condition \mathbf{p}_c does not intersect with the x -nullcline at $t \geq 0$. Hence, it is contained in Q_4 for $t \geq 0$ and its local expression is given by

$$\varphi(t; \mathbf{p}_c) = \varepsilon \begin{pmatrix} (C(\lambda) - 1)(e^{-t} - 1) - t \\ (\lambda + C(\lambda)) + t \end{pmatrix}$$

see equations in (17)-(18). Therefore, at time $\tau_c = \frac{\rho}{\varepsilon} + (C(\lambda) - 1)(e^{-\frac{\rho}{\varepsilon}} - 1)$, the solution satisfies that

$$\begin{aligned} \varphi(\tau_c; \mathbf{p}_c) &= \begin{pmatrix} \varepsilon(C(\lambda) - 1)(e^{-\frac{\rho}{\varepsilon} - (C(\lambda) - 1)(e^{-\frac{\rho}{\varepsilon}} - 1)} - 1) - \rho - \varepsilon(C(\lambda) - 1)(e^{-\frac{\rho}{\varepsilon}} - 1) \\ \varepsilon(\lambda + C(\lambda)) + \rho + \varepsilon(C(\lambda) - 1)(e^{-\frac{\rho}{\varepsilon}} - 1) \end{pmatrix} \\ &= \begin{pmatrix} -\rho + \varepsilon(C(\lambda) - 1)e^{-\frac{\rho}{\varepsilon}}(e^{-(C(\lambda) - 1)(e^{-\frac{\rho}{\varepsilon}} - 1)} - 1) \\ \rho + \varepsilon(\lambda + 1) + \varepsilon(C(\lambda) - 1)e^{-\frac{\rho}{\varepsilon}} \end{pmatrix}. \end{aligned}$$

Then,

$$\varphi(\tau_c; \mathbf{p}_c) - \begin{pmatrix} -\rho \\ \rho + \varepsilon(1 + \lambda) \end{pmatrix} = e^{-\frac{\rho}{\varepsilon}} \begin{pmatrix} \varepsilon(C(\lambda) - 1)(e^{(C(\lambda) - 1)(e^{-\frac{\rho}{\varepsilon}} - 1)} - 1) \\ \varepsilon(C(\lambda) - 1) \end{pmatrix}.$$

Since $\varepsilon \leq \varepsilon_0(\lambda)$, from (12) it follows that

$$d\left(\varphi(\tau_c; \mathbf{p}_c) - \begin{pmatrix} -\rho \\ \rho + \varepsilon(1 + \lambda) \end{pmatrix}\right) = O(e^{-\frac{\rho}{\varepsilon}}),$$

which ends the proof. \square

In the next Lemma we study the behaviour of the solution $\varphi(t; \mathbf{p}_a^-)$ for $\lambda \in (\ln(2), 1)$ after re-entering quadrant Q_4 . We take profit of the solutions through \mathbf{p}_t and \mathbf{p}_c described in Lemmas 5.2 and 5.4.

Lemma 5.5 *Fix $\lambda \in (\ln(2), 1)$ and set $0 < \varepsilon \leq \varepsilon_0(\lambda)$. Let $\varphi(t; \mathbf{p}_a^-)$ be the solution of system (2) with initial condition at \mathbf{p}_a^- . For $\tau = \tau_a + O(e^{-\frac{\rho}{\varepsilon}})$ with τ_a in Lemma 5.2, then $d(\varphi(\tau, \mathbf{p}_a^-), \mathcal{S}_{a,\varepsilon}^+ \cap \Delta_a^{\text{out}}) = O(e^{-\frac{\rho}{\varepsilon}})$.*

Proof: Notice that $\varphi(t; \mathbf{p}_a^-)$ is located between $\varphi(t - \lambda; \mathbf{p}_t)$ and $\varphi(t - (\lambda + C(\lambda)); \mathbf{p}_c)$ for $t > 0$. Therefore, the proof follows straightforwardly from Lemmas 5.2(b) and 5.4(b). \square

Next, we start the proof of the statement (b) of Theorem 3.1. To that aim, let us first consider the point $\mathbf{p}_\delta^{\text{in}} = (-\rho, -\rho + \varepsilon(1 - \lambda) + \delta) \in \Delta^{\text{in}}$. In order to reach Δ^{out} , we first need to integrate it until $y = 0$ (the change from quadrant Q_3 to quadrant Q_4). One can easily show that for $\tau = \frac{\rho + \delta}{\varepsilon} + 1 - \lambda$ we get

$$\varphi(\tau, \mathbf{p}_\delta^{\text{in}}) = \mathbf{p}_a^- + \delta e^{-\frac{\rho + \delta}{\varepsilon} + (1 - \lambda)} \mathbf{e}_1 \quad (13)$$

which is exponentially close to \mathbf{p}_a^- .

For $\lambda \leq \ln(2)$, following similar arguments than those in the proof of Lemma 5.2 we conclude that for $\tau = \frac{\rho + \delta}{\varepsilon} + 1 + \lambda$ then

$$d(\varphi(\tau, \mathbf{p}_a^- + \delta e^{-\frac{\rho + \delta}{\varepsilon} + (1 - \lambda)} \mathbf{e}_1), \mathcal{S}_{a,\varepsilon}^+ \cap \Delta_a^{\text{out}}) = O(e^{-\frac{\rho}{\varepsilon}}).$$

On the contrary, for $\ln(2) < \lambda < 1$, similarly as in the proof of Lemma 5.5, the solution $\varphi(t; \mathbf{p}_a^- + \delta e^{-\frac{\rho+\delta}{\varepsilon} + (1-\lambda)} \mathbf{e}_1)$ is located between the solutions $\varphi(t - \lambda; \mathbf{p}_t)$ and $\varphi(t - (\lambda + C(\lambda)); \mathbf{p}_c)$ for $t > 0$. Hence,

$$d(\varphi(\tau, \mathbf{p}_a^- + \delta e^{-\frac{\rho+\delta}{\varepsilon} + (1-\lambda)} \mathbf{e}_1), \mathcal{S}_{a,\varepsilon}^+ \cap \Delta_a^{\text{out}}) = O(e^{-\frac{\rho}{\varepsilon}}),$$

with $\tau = \tau_a + O(e^{-\frac{\rho}{\varepsilon}})$, which ends the proof of the statement (b) in Theorem 3.1.

5.1.2 Case $\lambda > 1$

Consider now the function $\varepsilon_1 : (1, +\infty) \rightarrow \mathbb{R}$ given by

$$\varepsilon_1(\lambda) = \min \left\{ \left(\frac{2(e^{\lambda-1} - 1)}{\rho + \lambda - 1} \right)^{\frac{1}{2}}, \frac{\rho}{2e^{\lambda-1} - (\lambda + 1)} \right\}. \quad (14)$$

Notice that for λ close to 1 the value of $\varepsilon_1(\lambda)$ is given by the first function in (14). As a consequence, $\lim_{\lambda \rightarrow 1} \varepsilon_1(\lambda) = 0$ and $\lim_{\lambda \rightarrow 1} \frac{d\varepsilon_1(\lambda)}{d\lambda} = -\infty$.

When $\lambda > 1$, the slow manifold $\mathcal{S}_{a,\varepsilon}^-$ leaves the region Q_3 at the point $\mathbf{p}_a^- = (0, \varepsilon(1 - \lambda))$, see expression (7). Hence, by following the flow in the region Q_2 , the solution through \mathbf{p}_a^- writes as

$$\varphi(t; \mathbf{p}_a^-) = \begin{pmatrix} 2\varepsilon(e^t - 1) - \varepsilon t \\ (1 - \lambda)\varepsilon + \varepsilon t \end{pmatrix},$$

see (17), for $t \in (0, \tau_1)$ where $\tau_1 := \lambda - 1$. Moreover, the solution $\varphi(t; \mathbf{p}_a^-)$ crosses from the quadrant Q_2 to the quadrant Q_1 through the point $\mathbf{p}_1 = \varphi(\tau_1; \mathbf{p}_a^-)$. In the next result we describe the behaviour of the solution through \mathbf{p}_1 .

Lemma 5.6 *Fix $\lambda > 1$ and set $0 < \varepsilon \leq \varepsilon_1(\lambda)$. Let $\varphi(t; \mathbf{p}_1)$ be the solution with initial condition at the point $\mathbf{p}_1 = (2\varepsilon e^{\lambda-1} - \varepsilon(1 + \lambda), 0)^\top$.*

- a) *For $t \geq 0$, the solution $\varphi(t; \mathbf{p}_1)$ is contained in the quadrant Q_1 .*
- b) *There exist functions $\tau(\varepsilon)$ and $h(\varepsilon)$ such that $\varphi(\tau(\varepsilon); \mathbf{p}_1) = (\rho, h(\varepsilon))^\top$, where $\tau(\varepsilon) = O(|\ln(\varepsilon)|)$ and $h(\varepsilon) = O(\varepsilon|\ln(\varepsilon)|)$.*

Proof: Notice that in the region of Q_1 limited by the coordinate axes and by the repelling slow manifold $\mathcal{S}_{r,\varepsilon}^+$, the vector field satisfies $\dot{x} > 0$ and $\dot{y} > 0$, see (2). Therefore, both coordinates of the solution $\varphi(t; \mathbf{p}_1)$ are strictly increasing and hence, it is contained in Q_1 for $t \geq 0$.

Let $x_1 = \varepsilon(2e^{\lambda-1} - (\lambda + 1)) > 0$ be the first coordinate of the point \mathbf{p}_1 . Since

$$\varepsilon < \varepsilon_1(\lambda) \leq \frac{\rho}{2e^{\lambda-1} - (\lambda + 1)},$$

it follows that $x_1 < \rho$. As both coordinates of the solutions are increasing with the time, there exist positive functions $\tau(\varepsilon)$ and $h(\varepsilon)$ such that $\varphi(\tau(\varepsilon); \mathbf{p}_1) = (\rho, h(\varepsilon))^\top$. Next, we study the order in ε of the functions $\tau(\varepsilon)$ and $h(\varepsilon)$.

Set $d = -\ln(\varepsilon^3) > 0$ and consider the first coordinate $x_d = (\rho - \varepsilon d + (\lambda - 1)\varepsilon)e^{-d} - (\lambda - 1)\varepsilon$, of the point \mathbf{p}_d introduced in Lemma A.1. Hence,

$$\begin{aligned} x_d &= (\rho + 3\varepsilon \ln(\varepsilon) + (\lambda - 1)\varepsilon)\varepsilon^3 - (\lambda - 1)\varepsilon \\ &< \varepsilon((\rho + \lambda - 1)\varepsilon^2 - \lambda + 1) \\ &\leq \varepsilon((\rho + \lambda - 1)\varepsilon_1^2(\lambda) - \lambda + 1) \\ &= \varepsilon(2e^{\lambda-1} - (\lambda + 1)), \end{aligned}$$

that is $x_d < x_1$. Consequently, it follows that the orbit defined by the solution $\phi(t; \mathbf{p}_d)$ introduced in Lemma A.1 bounds in Q_1 the orbit defined by $\varphi(t; \mathbf{p}_1)$, including their intersections with Δ_e^{out} . From Lemma A.1, we conclude that $h(\varepsilon) = O(\varepsilon|\ln(\varepsilon)|)$ and $\tau(\varepsilon) = O(|\ln(\varepsilon)|)$, which ends the proof. \square

Lemma 5.6 proves the first part of the statement (a) of Theorem 3.1. Next, we finish this proof. To that aim, let us consider the point $\mathbf{p}_\delta^{\text{in}} = (-\rho, -\rho + \varepsilon(1 - \lambda) + \delta) \in \Delta^{\text{in}}$. In order to reach Δ^{out} ,

we first need to integrate it until $x = 0$ (the change from quadrant Q_3 to quadrant Q_2). One can easily show that for $\tilde{\tau}_1 = \frac{\rho-\delta}{\varepsilon}$ we get

$$\varphi(\tilde{\tau}_1; \mathbf{p}_\delta^{\text{in}}) = \left(0, \varepsilon(1-\lambda) - \delta e^{-\frac{\rho-\delta}{\varepsilon}}\right)^\top = \mathbf{p}_a^- - \delta e^{-\frac{\rho-\delta}{\varepsilon}} \mathbf{e}_2, \quad (15)$$

which is exponentially close to \mathbf{p}_a^- .

Next, we compute the solution with initial condition at the point $\varphi(\tilde{\tau}_1; \mathbf{p}_\delta^{\text{in}})$ until it reaches the y -axis (where it changes from quadrant Q_2 to quadrant Q_1). Straightforward computations show that for $\tilde{\tau}_2 = \lambda - 1 + \frac{\delta}{\varepsilon} e^{-\tilde{\tau}_1}$ we get

$$\tilde{\mathbf{p}}_1 := \varphi(\tilde{\tau}_2; \varphi(\tilde{\tau}_1; \mathbf{p}_\delta^{\text{in}})) = \left((2\varepsilon - \delta e^{-\tilde{\tau}_1}) e^{\tilde{\tau}_2} - \varepsilon(\lambda + 1), 0\right)^\top. \quad (16)$$

Since $\frac{\delta}{\varepsilon} e^{-\tilde{\tau}_1}$ tends to zero with ε , we write

$$e^{\tilde{\tau}_2} = e^{\lambda-1} \left(1 + \frac{\delta}{\varepsilon} e^{-\tilde{\tau}_1} + O(e^{-2\tilde{\tau}_1})\right) = e^{\lambda-1} + \frac{\delta}{\varepsilon} e^{\lambda-1-\tilde{\tau}_1} + O(e^{-2\tilde{\tau}_1}),$$

and consequently

$$\tilde{\mathbf{p}}_1 = \mathbf{p}_1 + \left(\delta e^{\lambda-1-\tilde{\tau}_1} + O(e^{-2\tilde{\tau}_1}), 0\right)^\top,$$

where \mathbf{p}_1 is introduced in Lemma 5.6. We conclude that $\tilde{\mathbf{p}}_1$ and \mathbf{p}_1 are exponentially close and $\varphi(t; \tilde{\mathbf{p}}_1) \subset Q_1$ for $t > 0$. Therefore

$$\varphi(t; \tilde{\mathbf{p}}_1) = \varphi(t; \mathbf{p}_1) + \left((\delta e^{\lambda-1-\tilde{\tau}_1} + O(e^{-2\tilde{\tau}_1})) e^t, 0\right)^\top$$

for $t > 0$. In particular, for $t = \tau(\varepsilon)$ it follows that

$$\varphi(\tau(\varepsilon), \tilde{\mathbf{p}}_1) = \begin{pmatrix} \rho \\ h(\varepsilon) \end{pmatrix} + \begin{pmatrix} O(\frac{\delta}{\varepsilon} e^{-\tilde{\tau}_1}) \\ 0 \end{pmatrix}.$$

This ends the proof of the statement (a) of Theorem 3.1.

5.2 Proof of Theorem 3.6

When $\lambda = 1$, both slow manifolds do connect at the origin as it follows from the expression of $\mathcal{S}_{a,\varepsilon}^-$ and $\mathcal{S}_{r,\varepsilon}^+$ given in (5) and (6), respectively. Moreover, the slow manifolds lie on the straight line $y = x$, which is invariant under the flow. Therefore, the orbit through $\mathbf{p}_a^- = (0, 0)$ remains on the invariant set and thus the maximal delay is unbounded.

However, we may now discuss what happens with the points inside a neighbourhood N_δ around the slow-manifold. To do that, let us consider an orbit of the system entering the neighbourhood N_δ at a point $\mathbf{p}_i = (-\rho, -\rho + \delta)$. By following the flow we are interested in the point \mathbf{p}_o at which it leaves N_δ . Notice that, for $\tau_1 = \frac{\rho-\delta}{\varepsilon}$, then $\mathbf{p}_1 = \varphi(\tau_1; \mathbf{p}_i) = (-\delta e^{-\frac{\rho-\delta}{\varepsilon}}, 0)^\top$, see the expression of the flow in Q_3 given in (17)-(18). Moreover, there exists a time of flight

$$\tau_2 = \frac{\delta}{\varepsilon} e^{-\frac{\rho-\delta}{\varepsilon}} + O(e^{-2\frac{\rho-\delta}{\varepsilon}}),$$

such that

$$\mathbf{p}_2 = \varphi(\tau_2; \mathbf{p}_1) = \left(0, \delta e^{-\frac{\rho-\delta}{\varepsilon}} + O(e^{-2\frac{\rho-\delta}{\varepsilon}})\right).$$

Finally, for the times of flight

$$\tau_3 = \frac{\rho-\delta}{\varepsilon} - \frac{\delta}{\varepsilon} e^{-\frac{\rho-\delta}{\varepsilon}}, \quad \text{and} \quad \tau_4 = \frac{\rho}{\varepsilon} - \frac{\delta}{\varepsilon} e^{-\frac{\rho-\delta}{\varepsilon}}$$

we obtain

$$\varphi(\tau_3; \mathbf{p}_2) = \begin{pmatrix} \rho - \delta - \delta e^{-\frac{\delta}{\varepsilon} e^{-\frac{\rho-\delta}{\varepsilon}}} + O(e^{-\frac{\rho-\delta}{\varepsilon}}) \\ \rho - \delta + O(e^{-2\frac{\rho-\delta}{\varepsilon}}) \end{pmatrix} \quad \text{and} \quad \varphi(\tau_4; \mathbf{p}_2) = \begin{pmatrix} \rho - \delta e^{\frac{\delta}{\varepsilon}(1 - e^{-\frac{\rho-\delta}{\varepsilon}})} + O(e^{-\frac{\rho-\delta}{\varepsilon}}) \\ \rho + O(e^{-2\frac{\rho-\delta}{\varepsilon}}) \end{pmatrix}$$

Therefore, we conclude that the exit point \mathbf{p}_o has a second coordinate between $\rho - \delta$ and ρ . The same arguments apply if we consider $\mathbf{p}_i = (-\rho, -\rho - \delta)^\top$. This ends the proof of the theorem.

5.3 Proof of Theorem 3.8

In this Section we prove Theorem 3.8. Let us start with the statement (a). Assuming $c > 0$ and $\varepsilon > 0$ and small enough, the parameter $\lambda = 1 - e^{-\frac{c}{\varepsilon}}$ is greater than $\ln(2)$ and therefore the solution through \mathbf{p}_a^- evolves from quadrant Q_4 to Q_1 intersecting the y -axis at a point \mathbf{p}_1 below the tangent point \mathbf{p}_t . In particular, for the time of flight $\tau_1 = e^{-\frac{c}{\varepsilon}} + O(e^{-\frac{2c}{\varepsilon}})$ such that $\mathbf{p}_1 = \varphi(\tau_1; \mathbf{p}_a^-) = (0, y_1)^T$ with $y_1 = \varepsilon e^{-\frac{c}{\varepsilon}} + O(\varepsilon e^{-\frac{2c}{\varepsilon}})$, see equations (17)-(18). Moreover, for the time of flight $\tau_2 = \frac{c}{\varepsilon} + \ln(\frac{c}{2\varepsilon})$ such that $\varphi(\tau_2; \mathbf{p}_1) = (0 + X(\varepsilon), c + Y(\varepsilon))^T$ with

$$X(\varepsilon) = \varepsilon \ln\left(\frac{c}{2\varepsilon}\right) + O(\varepsilon e^{-\frac{c}{\varepsilon}}), \quad \text{and,} \quad Y(\varepsilon) = \varepsilon \ln\left(\frac{c}{2\varepsilon}\right) + O(e^{-\frac{c}{\varepsilon}}).$$

Let us now prove the statement (b). The parameter $\lambda = 1 + e^{-\frac{c}{\varepsilon}}$ is greater than 1 and therefore the solution through \mathbf{p}_a^- evolves from quadrant Q_3 to Q_1 intersecting the x -axis at a point \mathbf{p}_1 . In particular, there exists a time of flight $\tau_1 = e^{-c/\varepsilon}$ such that $\mathbf{p}_1 = \varphi(\tau_1; \mathbf{p}_a^-) = (x_1, 0)^T$ with $x_1 = \varepsilon e^{-c/\varepsilon} + O(e^{-2c/\varepsilon})$, see equations (17)-(18). Moreover, for $\tau_2 = \frac{c}{\varepsilon} + \ln(\frac{c}{2\varepsilon})$ it can be checked that $\varphi(\tau_2; \mathbf{p}_1) = (2c + X(\varepsilon), c + Y(\varepsilon))^T$ with

$$X(\varepsilon) = \varepsilon \ln\left(\frac{c}{2\varepsilon}\right) + O(\varepsilon e^{-\frac{c}{\varepsilon}}), \quad \text{and,} \quad Y(\varepsilon) = \varepsilon \ln\left(\frac{c}{2\varepsilon}\right).$$

6 Acknowledgements

AET is partially supported by the MCIU project PID2020-118726GB-I00 and by the Ministerio de Economía y Competitividad through the project MTM2017-83568-P (AEI/ERDF/EU). APC thanks the Departament de Matemàtiques i Informàtica of the UIB and the Instituto de Física Interdisciplinar y Sistemas Complejos (IFISC, UIB-CSIC) for hosting him during pandemic times.

References

- [1] S. M. Baer, T. Erneux, and J. Rinzel. The slow passage through a hopf bifurcation: Delay, memory effects, and resonance. *SIAM Journal on Applied Mathematics*, 49(1):55–71, 1989.
- [2] E. Benoit. Chasse au canard. *Collectanea Mathematica*, 32(2):37–119, 1981.
- [3] V. Carmona, S. Fernández-García, and A. E. Teruel. Birth, transition and maturation of canard cycles in a piecewise linear system with a flat slow manifold. *Physica D: Nonlinear Phenomena*, 443:133566, 2023.
- [4] V. Carmona, F. Fernández-Sánchez, and A. E. Teruel. Existence of a reversible t-point heteroclinic cycle in a piecewise linear version of the michelson system. *SIAM journal on applied dynamical systems*, 7(3):1032–1048, 2008.
- [5] V. Carmona, S. Fernández-García, and A. E. Teruel. Saddle-node canard cycles in planar piecewise linear differential systems. 2020.
- [6] P. de Maesschalck, F. Dumortier, and R. Roussarie. *Canard Cycles: from Birth to Transition*, volume 73 of *Ergebnisse der Mathematik und ihrer Grenzgebiete. 3. Folge / A Series of Modern Surveys in Mathematics*. Springer International Publishing, 2021.
- [7] M. Desroches, S. Fernández-García, M. Krupa, R. Prohens, and A. E. Teruel. Piecewise-linear (pwl) canard dynamics - simplifying singular perturbation theory in the canard regime using piecewise-linear systems. In V. Carmona, J. Cuevas-Maraver, F. Fernández-Sánchez, and E. García-Medina, editors, *Nonlinear Systems, Vol. 1: Mathematical Theory and Computational Methods*, pages 67–86. Springer International Publishing, Cham, 2018.
- [8] M. Desroches, A. Guillamon, E. Ponce, R. Prohens, S. Rodrigues, and A. E. Teruel. Canards, folded nodes, and mixed-mode oscillations in piecewise-linear slow-fast systems. *SIAM Review*, 58(4):653–691, 2016.
- [9] M. Diener. Regularizing microscopes and rivers. *SIAM Journal on Mathematical Analysis*, 25(1):148–173, 1994.

- [10] M. Engel and C. Kuehn. Discretized fast-slow systems near transcritical singularities. Nonlinearity, 32(7):2365, may 2019.
- [11] T. Erneux, E. L. Reiss, L. J. Holden, and M. Georgiou. Slow passage through bifurcation and limit points. asymptotic theory and applications. In E. Benoît, editor, Dynamic Bifurcations, pages 14–28, Berlin, Heidelberg, 1991. Springer Berlin Heidelberg.
- [12] N. Fenichel. Geometric singular perturbation theory for ordinary differential equations. Journal of Differential Equations, 31(1):53–98, 1979.
- [13] S. Fernández-García, M. Desroches, M. Krupa, and A. Teruel. Canard solutions in planar piecewise linear systems with three zones. Dynamical Systems An International Journal, 31:173–197, 08 2016.
- [14] A. F. Filippov. Differential equations with discontinuous righthand sides: control systems, volume 18. Springer Science & Business Media, 2013.
- [15] J.-P. Francoise, C. Piquet, and A. Vidal. Enhanced delay to bifurcation. Bulletin of the Belgian Mathematical Society-Simon Stevin, 15(5):825–831, 2008.
- [16] M. Guardia, T. Seara, and M. A. Teixeira. Generic bifurcations of low codimension of planar filippov systems. Journal of Differential equations, 250(4):1967–2023, 2011.
- [17] R. Haberman. Slowly varying jump and transition phenomena associated with algebraic bifurcation problems. SIAM Journal on Applied Mathematics, 37(1):69–106, 1979.
- [18] R. Haberman. Slow passage through a transcritical bifurcation for hamiltonian systems and the change in action due to a nonhyperbolic homoclinic orbit. Chaos: An Interdisciplinary Journal of Nonlinear Science, 10(3):641–648, 2000.
- [19] M. G. Hayes, T. J. Kaper, P. Szmolyan, and M. Wechselberger. Geometric desingularization of degenerate singularities in the presence of fast rotation: A new proof of known results for slow passage through Hopf bifurcations. Indagationes Mathematicae, 27(5):1184–1203, 2016.
- [20] C. K. R. T. Jones. Geometric singular perturbation theory, pages 44–118. Springer Berlin Heidelberg, Berlin, Heidelberg, 1995.
- [21] P. Kaklamanos, C. Kuehn, N. Popović, and M. Sensi. Entry–exit functions in fast–slow systems with intersecting eigenvalues. Journal of Dynamics and Differential Equations, pages 1–18, 2023.
- [22] M. Krupa and P. Szmolyan. Extending slow manifolds near transcritical and pitchfork singularities. Nonlinearity, 14(6):1473, 2001.
- [23] N. Lebovitz and R. Schaar. Exchange of stabilities in autonomous systems. Studies in Applied Mathematics, 54(3):229–260, 1975.
- [24] N. Lebovitz and R. Schaar. Exchange of stabilities in autonomous systems—ii. vertical bifurcation. Studies in Applied Mathematics, 56(1):1–50, 1977.
- [25] J. Llibre, E. Ponce, and A. E. Teruel. Horseshoes near homoclinic orbits for piecewise linear differential systems in \mathbf{R}^3 . International Journal of Bifurcation and Chaos, 17(04):1171–1184, 2007.
- [26] A. Neishtadt. Persistence of stability loss for dynamical bifurcations i. Differential Equations, 23:1385–1391, 1987.
- [27] A. Neishtadt. Persistence of stability loss for dynamical bifurcations ii. Differential Equations, 24:171–176, 1988.
- [28] J. Penalva, M. Desroches, A. E. Teruel, and C. Vich. Slow passage through a hopf-like bifurcation in piecewise linear systems: Application to elliptic bursting. Chaos: An Interdisciplinary Journal of Nonlinear Science, 32(12):123109, 2022.
- [29] J. Penalva, M. Desroches, A. E. Teruel, and C. Vich. Dynamics of a piecewise-linear morris-lecar model: bifurcations and spike adding. arXiv, 2023.

- [30] E. Ponce, J. Ros, and E. Vela. Bifurcations in Continuous Piecewise Linear Differential Systems: Applications to Low-Dimensional Electronic Oscillators, volume 7. Springer Nature, 2022.
- [31] R. Prohens, A. Teruel, and C. Vich. Slow-fast n -dimensional piecewise linear differential systems. Journal of Differential Equations, 260(2):1865–1892, jan 2016.
- [32] A. Vidal and J.-P. Françoise. Canard cycles in global dynamics. International Journal of Bifurcation and Chaos, 22(02):1250026, 2012.

A Local expressions for the flow

We provide local expressions for the flow $\varphi(t; (x_0, y_0), \lambda, \varepsilon)$ of the PWL normal form (2) depending on (x_0, y_0) is located in each of the four quadrants of the phase-space, which we denote by Q_i (with $i = 1, \dots, 4$) following the clockwise convention. For simplify notation, when no confusion arises we will avoid make explicit the dependence of the flow with respect to the parameters λ and ε . In particular, the first coordinate of the flow is given by

$$\varphi_1(t; (x_0, y_0)) = \begin{cases} (x_0 - y_0 + (\lambda - 1)\varepsilon)e^t + \varepsilon t + y_0 - (\lambda - 1)\varepsilon & (x_0, y_0) \in Q_1, \\ (x_0 + y_0 + (1 + \lambda)\varepsilon)e^t - \varepsilon t - y_0 - (\lambda + 1)\varepsilon & (x_0, y_0) \in Q_2, \\ (x_0 - y_0 + (1 - \lambda)\varepsilon)e^{-t} + \varepsilon t + y_0 + (\lambda - 1)\varepsilon & (x_0, y_0) \in Q_3, \\ (x_0 + y_0 - (1 + \lambda)\varepsilon)e^{-t} - \varepsilon t - y_0 + (\lambda + 1)\varepsilon & (x_0, y_0) \in Q_4, \end{cases} \quad (17)$$

whereas the second coordinate is given by

$$\varphi_2(t; (x_0, y_0)) = y_0 + \varepsilon t. \quad (18)$$

Here we introduce the following technical result.

Lemma A.1 *Consider the linear differential system $\dot{x} = x - y + \varepsilon\lambda$, $\dot{y} = \varepsilon$ defined in whole \mathbb{R}^2 , and let $\phi(t; \mathbf{p})$ be the solution with initial condition at the point $\mathbf{p}_d = ((\rho - \varepsilon d + (\lambda - 1)\varepsilon)e^{-d} - (\lambda - 1)\varepsilon, 0)^\top$ with $d > 0$. Then, $\phi(d; \mathbf{p}_d) = (\rho, \varepsilon d)^\top$.*

Proof: The proof follows by direct computations from the expression of the flow in Q_1 given in (17) – (18). \square